frontiers | Frontiers in Energy Research

TYPE Original Research
PUBLISHED 02 June 2023
DOI 10.3389/fenrg.2023.1212664

OPEN ACCESS

EDITED BY
Chengyuan Xu,
Southwest Petroleum University, China

REVIEWED BY
Peng Xu,
China Jiliang University, China
Maje Alhaji Haruna,
University of Leeds, United Kingdom
Jinzi Liu,
Northeast Petroleum University, China

*CORRESPONDENCE
Yunqian Long,
longyunqian@zjou.edu.cn

RECEIVED 26 April 2023
ACCEPTED 23 May 2023
PUBLISHED 02 June 2023

CITATION
Hu X, Long Y, Xuan G, Wang Y, Huang X, Xu Y, Liu J, Wang B and Song F (2023), Optimized hydrophobic magnetic nanoparticles stabilized pickering emulsion for enhanced oil recovery in complex porous media of reservoir. *Front. Energy Res.* 11:1212664. doi: 10.3389/fenrg.2023.1212664

Optimized hydrophobic magnetic nanoparticles stabilized pickering emulsion for enhanced oil recovery in complex porous media of reservoir

Xiaojuan Hu[1], Yunqian Long[1,2]*, Gong Xuan[3], Yuyi Wang[1], Xiaohe Huang[1,2], Yupeng Xu[1,2], Jing Liu[4], Bohong Wang[2] and Fuquan Song[5]

[1]College of Petrochemical Engineering and Environment, Zhejiang Ocean University, Zhoushan, China, [2]National and Local Joint Engineering Research Center of Harbor Oil and Gas Storage and Transportation Technology, Zhejiang Ocean University, Zhoushan, China, [3]China National Logging Corporation, Xi'an, China, [4]Foundation College, Zhejiang Pharmaceutical University, Ningbo, China, [5]College of Petroleum and Nature Gas Engineering and College of Energy, Changzhou University, Changzhou, China

With an extensive application of flooding technologies in oil recovery, traditional emulsion flooding has seen many limits due to its poor stability and easy demulsification. Pursuing a new robust emulsion plays a fundamental role in developing highly effective emulsion flooding technology. In this work, a novel Pickering emulsion with special magnetic nanoparticles Fe_3O_4@PDA@Si was designed and prepared. To disclose the flooding mechanism from magnetic nanoparticles, the physico-chemical characterization of Fe_3O_4@PDA@Si was systematically examined. Meanwhile, the flooding property of the constructed Pickering emulsion was evaluated on the basis of certain downhole conditions. The results showed that the synthesis of Fe_3O_4@PDA@Si nanoparticles was found to have a hydrophobic core-shell structure with a diameter of 30 nm. Pickering emulsions based on Fe_3O_4@PDA@Si nanoparticles at an oil-to-water ratio of 5:5, 50°C, the water separation rate was only 6% and the droplet diameter of the emulsion was approximately 15 μm in the ultra-depth-of-field microscope image. This demonstrates the excellent stability of Pickering emulsions and improves the problem of easy demulsification. We further discussed the oil displacement mechanism and enhanced oil recovery effect of this type of emulsion. The microscopic flooding experiment demonstrated that profile control of the Pickering emulsion played a more important role in enhanced recovery than emulsification denudation, with the emulsion system increasing oil recovery by 10.18% in the micro model. Core flooding experiments have established that the incremental oil recovery of the Pickering emulsion increases with decreasing core permeability, from 12.36% to 17.39% as permeability drops from 834.86 to 219.34 × 10^{-3} μm^2. This new Pickering emulsion flooding system stabilized by Fe_3O_4@PDA@Si nanoparticles offers an option for enhanced oil recovery (EOR).

KEYWORDS

pickering emulsion, Fe3O4@PDA@Si nanoparticles, profile control, emulsification denudation, enhanced oil recovery

1 Introduction

Oil as one of the world's major energy resources is vital to ensuring energy security and promoting economic development. However, in the water injection development stage of oil reservoirs, the oil recovery efficiency sharply decreases due to the breakthrough of the water flooding front caused by the viscous fingering of the injected water in the high permeability areas of oil reservoirs (Long et al., 2019a; Suleimanov et al., 2022). Therefore, it is urgent to improve oil recovery from reservoirs after water injection development in order to exploit oil resources more effectively, improve the efficiency of oil resources utilization, reduce resource waste and meet global energy demand and economic development (Long et al., 2019b; Gogoi and Gogoi, 2019). Among numerous methods for improving oil recovery, the emulsion flooding technology has been much concerned by the public (Carvalho and Alvarado, 2014; Cheraghian et al., 2020). Since the emulsion flooding technology was applied in practical oil fields in the last century, it has been confirmed via a large number of lab experiments and oilfield practices that the emulsion has played an important role in improving oil recovery and can achieve an enhanced oil recovery of more than 10% (Cao et al., 2022; Tiong et al., 2023).

In the past few decades, many scholars (Jia et al., 2021a; Liang et al., 2022) have conducted extensive research on the stability of traditional emulsion and its influencing factors, emulsification mechanism, and mechanism of improving recovery efficiency. (Bai et al., 2014) found that surfactant concentration, chemical slug size, slug type, and experimental temperature all have an impact on incremental oil recovery of the emulsion flooding. Due to the synergistic effect of the surfactant at the oil/water interface, the oil/water interfacial tension is reduced, the oil phase can be more easily emulsified and dispersed, and the stability of the emulsion can be enhanced. (Carvalho and Alvarado, 2014) utilized reservoir simulators to confirm that emulsion flooding can improve displacement efficiency at the pore scale (Zhou et al., 2019). Analyzed the formation mechanism, rheology, stability, and seepage characteristics of the emulsion and summarized the mechanisms of enhanced oil recovery by emulsification. (Mehranfar and Ghazanfari, 2014) conducted the emulsion flooding experiments using glass micromodels with randomly distributed shale cracks and analyzed various mechanisms of improving heavy oil recovery during emulsion flooding. The results show that the injected water-in-oil (W/O) emulsion increases the swept area, reduces the viscous fingering effect, and extends the breakthrough time of the water phase, leading to a significant increase in enhanced oil recovery (AfzaliTabar et al., 2017; Namin et al., 2023). It is thus clear that the oil displacement mechanism of traditional emulsion forms tiny oil-water particles between water and oil phases using an emulsifier to increase surface area, reduce pore pressure, and decrease relative permeability, so as to achieve the purpose of improving oil recovery. However, traditional emulsions have disadvantages including poor stability, easy layering, high viscosity, and difficulty in demulsification (Umar et al., 2018). Therefore, in order to overcome these shortcomings, it is urgent to develop a new emulsion system.

Compared with traditional emulsion, Pickering emulsion is a new type of emulsion system, which is stabilized by solid particles or nanoparticles instead of traditional organic surfactants as emulsifiers (Wu and Ma, 2016; Xu et al., 2022). It has unique physical and chemical properties, such as strong stability, extensive sources, etc. Therefore, Pickering emulsion has gradually been applied in oil fields. Relying on the special stability mechanism of Pickering emulsion, appropriate solid particles can be selected to prepare Pickering emulsions that can respond to different environments to solve issues such as poor stability and difficulty in demulsification encountered during the process of improving oil recovery (Zhu et al., 2021; Li W. et al., 2022). Magnetic responsive emulsion (magnetic emulsion), which is stabilized by magnetic particles as an emulsifier, can realize directional movement under the action of the external magnetic field (Kazemzadeh et al., 2018; Li X. et al., 2022). Thus, the magnetic Pickering emulsion can be used to simultaneously solve the problems of poor stability of the emulsion and difficulty in demulsification of the produced liquid encountered during the emulsion flooding.

Among numerous magnetic materials, Fe_3O_4 nanoparticles have been widely used to prepare magnetically responsive Pickering emulsion due to their excellent magnetic property (Niebel et al., 2014; Zhou et al., 2014; Zhao et al., 2022). Currently, some domestic and foreign scholars have conducted some exploratory studies in enhanced oil recovery using the magnetically responsive emulsion stabilized by Fe_3O_4 nanoparticles. (Sharma et al., 2016) found via core displacement experiments that particle morphology and size, surface property, concentration, emulsion droplet size, interaction forces, and flow state all had an influence on the stability of the emulsion, thus affecting the effect of improving oil recovery. The emulsion stabilized by Fe_3O_4/SiO_2 nanoparticles (0.1 wt%) could improve oil recovery by 13.2% in the microscopic flooding experiments. (Yakasai et al., 2023) thought that the emulsion stabilized by nanoparticles could block high-permeability pores in the reservoir during displacement to improve sweep efficiency, and the enhanced oil recovery increased with an increase in the emulsion stability. The emulsion stabilized by iron oxide nanoparticles functionalized with 3-aminopropyltriethoxysilane could improve oil recovery by 13.3% in core flooding experiments. (Shalbafan et al., 2020) investigated the influence of particle size, shape, and surface modification on the emulsification effect, explored the influence of the interaction between solid particles and the oil-water phases on enhanced oil recovery, and found that the emulsions stabilized by Fe_3O_4 nanoparticles covered with polyvinyl pyrrolidone (PVP) and sodium dodecyl sulfate (SDS) improved the oil recovery by 16.0% and 13.0%, respectively. (Rezvani et al., 2019) prepared the W/O emulsion stabilized by Fe_3O_4 nanoparticles modified with chitosan. Compared with the emulsion stabilized by Fe_3O_4 nanoparticles, the above emulsion had a higher viscosity of 334.0 mPa s·and could form a more uniform plugging in the pores. Core displacement experiments on sandstones confirmed that the emulsion prepared using hydrophobically modified Fe_3O_4 nanoparticles could increase the sweep efficiency and improve oil recovery by 15.0%. Currently, the oil-in-water (O/W) emulsions stabilized by Fe_3O_4 nanoparticles still have certain deficiencies in stability and viscosity (Gbadamosi et al., 2018; Kazemzadeh et al., 2019). To further improve the stability and viscosity of the emulsions stabilized by Fe_3O_4 nanoparticles, it is necessary to modify the surface of Fe_3O_4 nano-particles and improve their hydrophobicity to prepare a stable W/O emulsion with higher viscosity, which will be more conducive to further improving the

TABLE 1 Basic parameters of the artificial cores used in the flooding experiments.

Core no.	Length (cm)	Diameter (cm)	Permeability (10^{-3} μm^2)	Porosity (%)
1	2.52	5.35	219.34	21.05
2	2.54	5.47	365.28	23.89
3	2.51	5.19	537.92	24.63
4	2.57	5.27	834.86	24.27

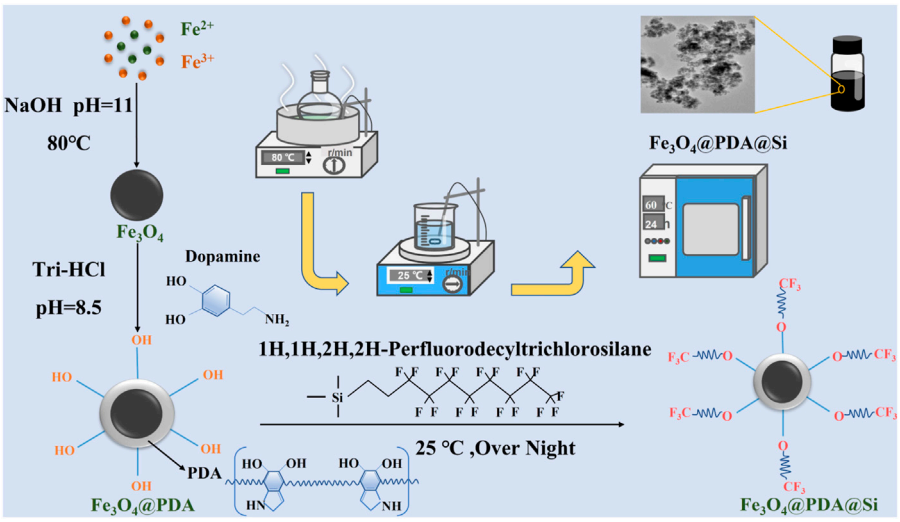

FIGURE 1
Schematic illustration of the synthetic route of Fe_3O_4@PDA@Si nanoparticles.

sweep efficiency during the displacement process, thus improving oil recovery.

This study is to propose a new emulsion flooding system using Fe_3O_4@PDA@Si nanoparticles to improve oil recovery from reservoirs after water injection development. Firstly, the magnetic Fe_3O_4 nanoparticles were synthesized by the coprecipitation method (Su et al., 2015). Hydrophobic Fe_3O_4@PDA@Si nanoparticles were prepared by coating dopamine (DA) and modifying with 1H, 1H, 2H, 2H-perfluorodecyltrichlorosilane on the surface of Fe_3O_4 nanoparticles. The morphology, composition, structure, and contact angle of Fe_3O_4@PDA@Si nanoparticles were characterized by transmission electron microscope (TEM), X-ray diffractometer (XRD), Fourier infrared spectrometer (FTIR), and contact angle tester (WCA). Subsequently, the Pickering emulsion stabilized by Fe_3O_4@PDA@Si nanoparticles was prepared using a high-speed dispersing homogenizer and its stability was evaluated. In addition, the microscopic displacement mechanism of the Pickering emulsion was investigated using an etched glass model as a porous medium to carry out microscopic flooding experiments. Core-flooding experiments were conducted to investigate the ability of enhanced oil recovery of the Pickering emulsion. This work will provide a better understanding of the microscopic displacement mechanism of Pickering emulsions in complex porous media of reservoir and explore more efficient reservoir recovery methods to improve oil recovery. Meanwhile, the magnetic Pickering emulsion flooding technique, as an improved reservoir recovery technique, can contribute to the efficient recovery of oil resources by enabling efficient oil recovery in mature oil fields. Therefore, the results of this study can provide effective theoretical and technical support for scientific research and engineering practice related to enhanced oil recovery (EOR).

2 Materials and methods

2.1 Materials

For requirements for a specific article type Anhydrous ethanol, sodium hydroxide, ferrous sulfate heptahydrate, ferric chloride hexahydrate, and trisodium citrate dihydrate were purchased from Sinopharm Group Chemical Reagent Co., Ltd. (China) for the preparation of Fe_3O_4 nanoparticles. Dopamine hydrochloride (98%) (DA), 1H, 1H, 2H, 2H-perfluorodecyltrichlorosilane, and n-hexane were purchased from Shanghai McLean Biochemical Technology Co., Ltd. (China) for the synthesis of Fe_3O_4@PDA@Si nanoparticles. Sodium carbonate, sodium bicarbonate, sodium sulfate, sodium chloride, magnesium chloride, and calcium chloride were purchased from Sinopharm Chemical Reagent Co., Ltd.

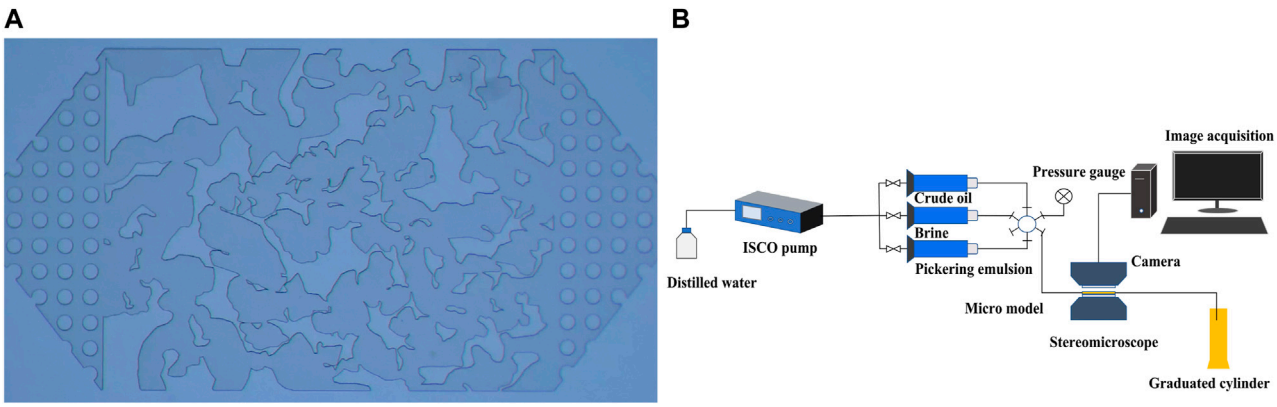

FIGURE 2
(A) Photograph of the etched glass micromodel. **(B)** The flow diagram of the microscopic flooding experiment.

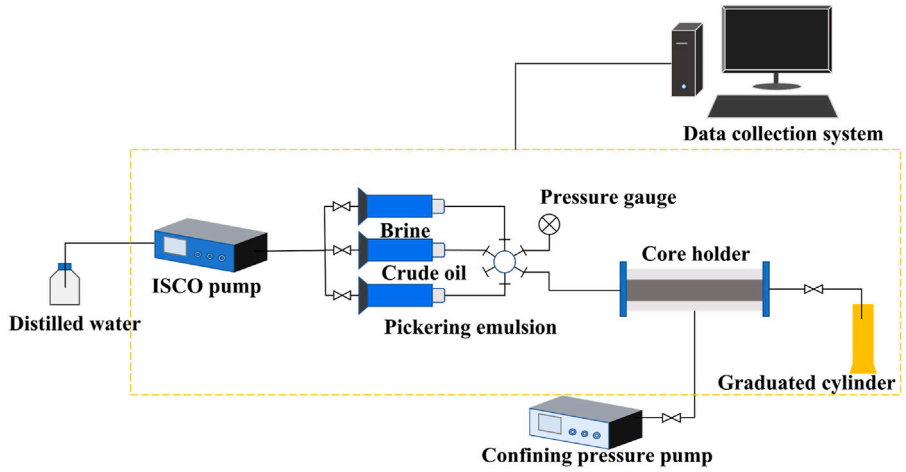

FIGURE 3
Flow diagram of the core flooding experiment.

(China) to prepare the simulated formation water. All the chemical reagents were of analytical grade and all solutions were prepared in deionized water. The synthetic formation water was brine with a total dissolved solids (TDS) value of 5,260 ppm and was used in all flow tests. The crude oil with a density of 0.8569 g/cm^3 and a viscosity of 7.69 mPa s (50°C) was obtained from the Daqing oil reservoir. The artificial cores were used in the flooding experiments and their basic parameters are shown in Table 1.

2.2 Synthesis of Fe_3O_4 nanoparticles

Fe_3O_4 nanoparticles were synthesized by the coprecipitation method. $FeSO_4{\cdot}7H_2O$ (5.56 g) and $FeCl_3{\cdot}6H_2O$ (5.41 g) were dissolved in the deionized water (100 mL). The mixture was stirred for 30 min at 60°C, and the NaOH solution (1 mol/L) was added to the mixture drop by drop until the pH value of the mixture was up to 11. After the trisodium citrate was added to the reaction solution, the solution was stirred for 1 h at 80°C and then cooled down to room temperature. The products were washed with distilled water and anhydrous ethanol until the pH value of the solution was down to 7. After that, the products were dried for 12 h at 60°C and were ground to obtain the Fe_3O_4 nanoparticles.

2.3 Synthesis of Fe_3O_4@PDA nanoparticles

Tris-HCl buffer solution with the pH value of 8.5 was prepared. Fe_3O_4 nanoparticles (0.5 g) were added to the Tris-HCl buffer solution (150 mL) and dispersed evenly by ultrasonic method. DA (0.3 g) was added to the previous solution and stirred for 12 h at 25°C. The products were collected by a magnet washed with deionized water and anhydrous ethanol, Vacuum dried for 12 h at 60°C, and ground to obtain Fe_3O_4@PDA nanoparticles.

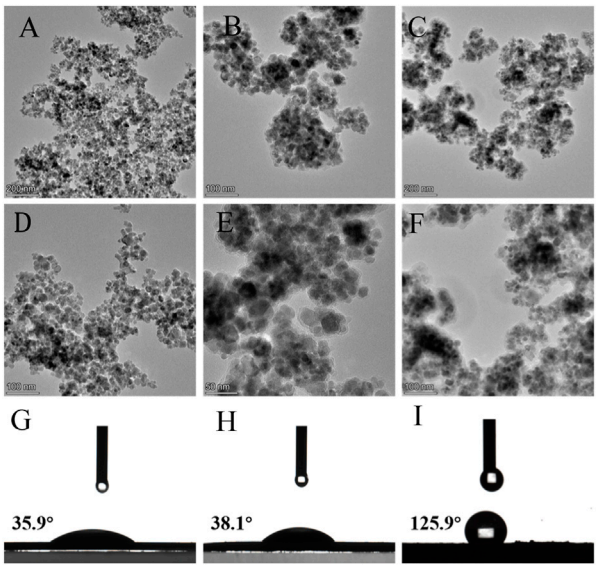

FIGURE 4
(A, D) TEM images of Fe_3O_4. **(B, E)** TEM images of Fe_3O_4@PDA. **(C, F)** TEM images of Fe_3O_4@PDA@Si nanoparticles. **(G)** WCA images of Fe_3O_4. **(H)** WCA images of Fe_3O_4@PDA. **(I)** WCA images of Fe_3O_4@PDA@Si nanoparticles.

2.4 Synthesis of Fe_3O_4@PDA@Si nanoparticles

1H, 1H, 2H, 2H-perfluorodecyltrichlorosilane (5 μL) was added to n-hexane and stirred for 10 min Fe_3O_4@PDA nanoparticles were poured into the mixed solution (150 mL) and stirred for 24 h at room temperature. The products were collected by a magnet washed with deionized water and anhydrous ethanol, dried for 12 h at 60°C, and ground to obtain Fe_3O_4@PDA@Si nanoparticles. The synthesis route of Fe_3O_4@PDA@Si nanoparticles is shown in Figure 1.

2.5 Preparation of pickering emulsion stabilized by Fe_3O_4@PDA@Si nanoparticles

Fe_3O_4@PDA@Si nanoparticles (5 g) were added into deionized water (1 L), and sonicated for 10 min. Then, the above solution and crude oil were mixed according to a certain oil-water ratio (1:9, 2:8, 3:7; 4:6, and 5:5). The mixture was dispersed for 10 min at 7,000 r/min by a high-speed dispersing homogenizer (T18, IKA Co., Ltd., Germany) to prepare a water-in-oil (W/O) Pickering emulsion stabilized by Fe_3O_4@PDA@Si nanoparticles.

2.6 Characterization

The morphologies of Fe_3O_4, Fe_3O_4@PDA, and Fe_3O_4@PDA@Si nanoparticles were observed by a transmission electron microscope (TEM, FEI TF20, Zeiss, Germany). The contact angle tester (WCA, JY-82B, Cruise, Germany) was used to determine the wettability of water droplets on the surface of Fe_3O_4, Fe_3O_4@PDA, and Fe_3O_4@PDA@Si nanoparticles. The X-ray diffractometer (XRD, Ultima IV, Rigaku Co., Ltd., Japan) was applied to measure the crystal structure of Fe_3O_4, Fe_3O_4@PDA, and Fe_3O_4@PDA@Si nanoparticles with a wavelength of 1.5406 nm, a scanning range of 5°–90°, and a scanning speed of 5°/min. The Fourier infrared spectrometer (FTIR, Nicolet iS20, Thermo Fisher Scientific, China) was used to analyze the functional group and chemical bond of Fe_3O_4 Fe_3O_4@PDA, and Fe_3O_4@PDA@Si nanoparticles in the range of 4,000–400 cm^{-1}.

2.7 Stability evaluation of pickering emulsion stabilized by Fe_3O_4@PDA@Si nanoparticles

The prepared Pickering emulsions (10 mL) with different oil-water ratios (1:9, 2:8, 3:7; 4:6, and 5:5) were poured into five graduated test tubes, respectively. Then, the five graduated test tubes with the Pickering emulsions were placed in a thermostatic water bath at 50°C. The volume of water evolved from the Pickering emulsion was continuously recorded in each test tube until the volume of water remains constant. According to the final volume of the evolved water, the water separating proportion (f) can be calculated as follow:

$$f = \frac{V_1}{V_2} \times 100\% \quad (1)$$

Where, the V_1 is the final volume of the evolved water, mL; the V_2 is the total volume of the water phase in the Pickering emulsion, mL.

In addition, a drop of freshly prepared Pickering emulsion was taken using a dropper and slowly dropped onto a slide. Then, the droplet of the Pickering emulsion was gently covered using a coverslip. When the droplet of the Pickering emulsion was evenly spread on the slide, the type of the Pickering emulsion and the distribution of oil and water were observed, the particle sizes of the Pickering emulsion droplets were measured, and the microscopic photos of the Pickering emulsion were recorded using a super depth of field optical microscope (VHX-5000, Keyence, Japan).

2.8 Microscopic flooding experiment

The microscopic flooding experiment was carried out by using an etched glass micromodel as the porous medium. Microscopic flooding experiment using etched glass micro-models as porous media. Based on the realistic pore structure of natural cores from the Daqing oilfield, photo-chemical methods were used to, etch the pore network on a glass plate. A micro-model of the etched glass plate was made by sintering the etched glass plate with another smooth glass plate. On both sides of the smooth glass, small holes were drilled to simulate injection and production wells in the reservoir. The porosity of the glass micro-model was 25%. The pore inner diameter is in the range of 30–200 μm in the etched glass micromodel, as shown in Figure 2A. The process of the microscopic displacement experiment is shown in Figure 2B. The experimental setup includes three containers with different fluids, a micro constant speed pump, a visual observation system and an image acquisition system, and a measuring cylinder for collecting fluid at the outlet. First, the micromodel was dried at 120°C for 24 h after washing with distilled water, and weighed to obtain the dry weight. The dried micromodel was vacuumed using a vacuum

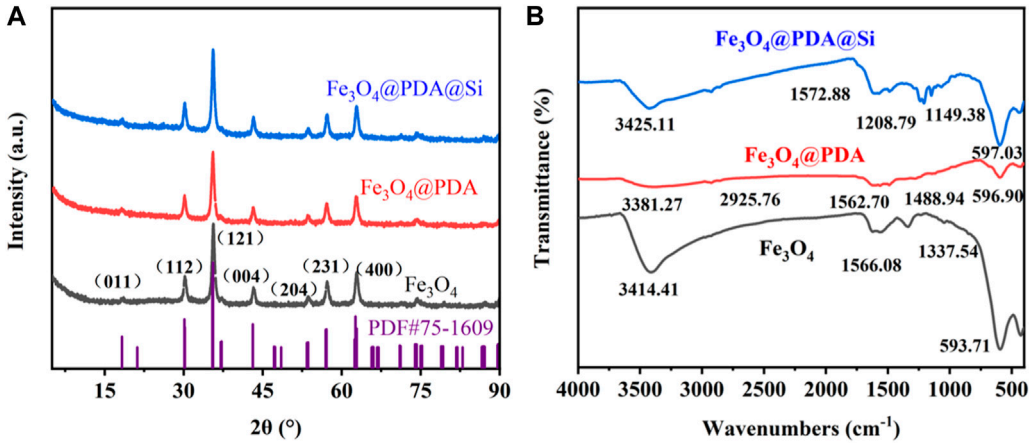

FIGURE 5
(A) XRD patterns of Fe_3O_4, Fe_3O_4@PDA, and Fe_3O_4@PDA@Si nanoparticles. **(B)** FTIR spectra of Fe_3O_4, Fe_3O_4@PDA, and Fe_3O_4@PDA@Si nanoparticles.

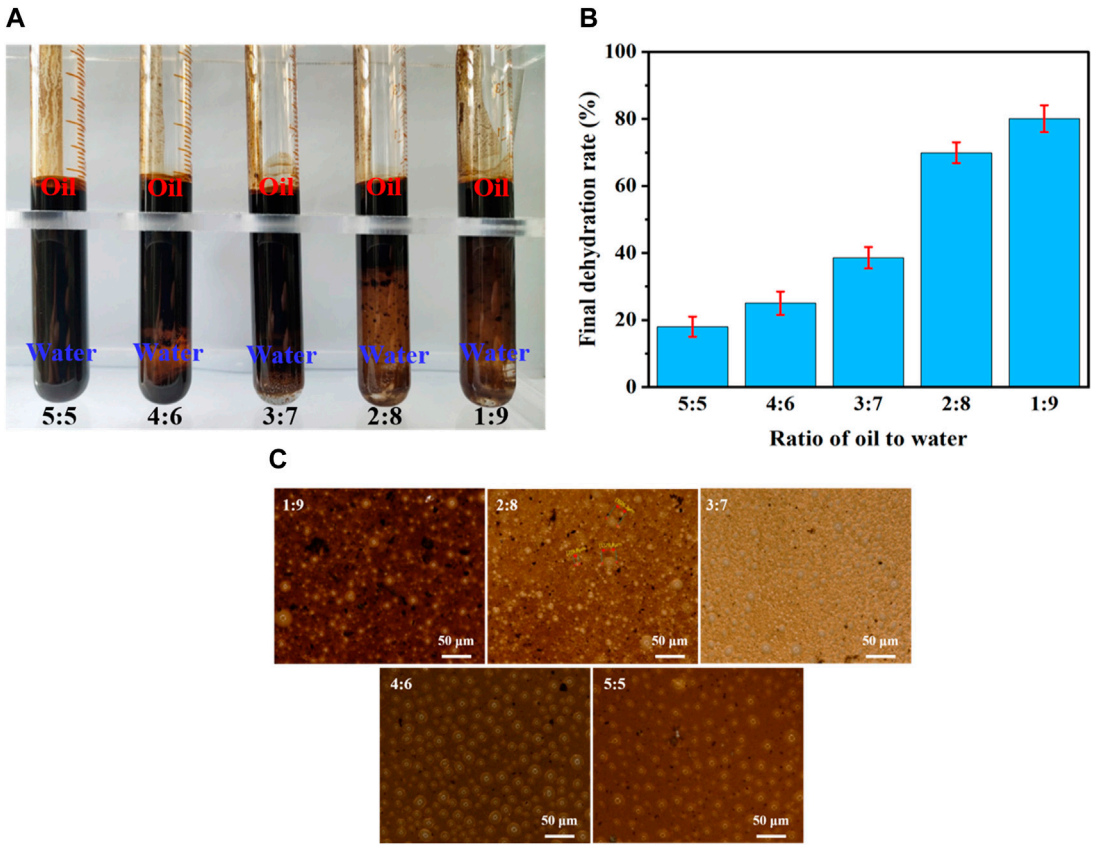

FIGURE 6
(A) Macroscopic photos. **(B)** The water separating proportion. **(C)** Microscopic photos of the Pickering emulsions with different oil-water ratios.

pump, saturated with simulated formation water using a flow pump, and weighed to obtain the wet weight again. The porosity of the micromodel was calculated by the weight method according to the wet and dry weight of the micromodel. Then, the water volume was determined at the outlet end of the micromodel to calculate the initial oil saturation when the crude oil was injected into the

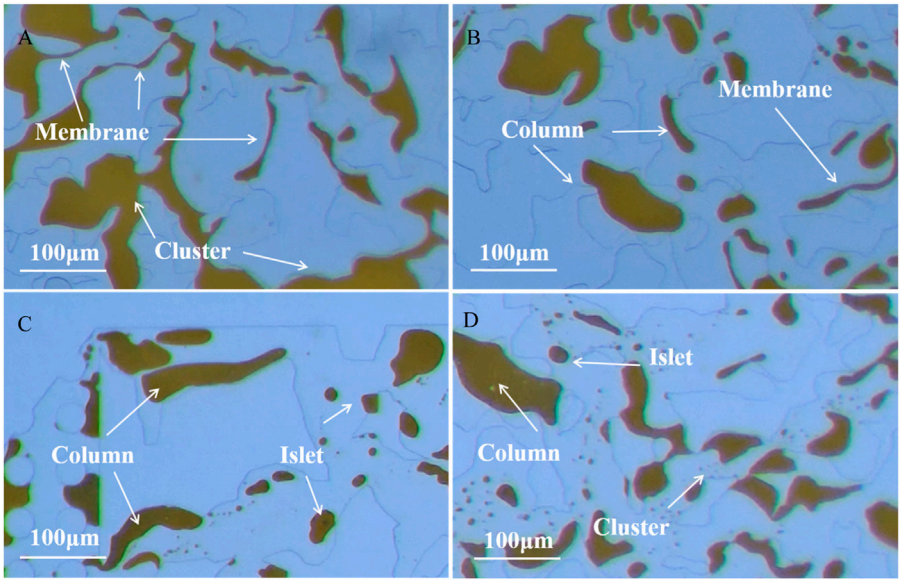

FIGURE 7
Morphology of residual oil after water flooding at different pores in the micromodel: residual oil in the membrane **(A, B)**, column **(B, C, D)**, and islet **(C, D)** forms in large pores, and residual oil in the cluster **(A, D)** form in small pores.

micromodel. The micromodel saturated with crude oil was aged for 24 h at 50°C to obtain the ideal wettability. After that, the aged micromodel was flooded with the simulated formation water at an injection rate of 0.1 mL/min, a slug of Pickering emulsion (0.3 PV, pore volume) was injected at the residual oil saturation of water flooding, and then the extended waterflood was performed after the injection of Pickering emulsion was completed. The images of the microscopic displacement were continuously recorded during the flooding experiment. In order to achieve the oil saturation from the residual oil images, the images were sharpened to improve the contrast. Then, the water and oil in the images were discriminated by the gray thresholds according to a program developed using Python. Finally, the oil saturation was obtained via calculating the area ratio of oil to pore space.

2.9 Core-flooding experiment

The process of the core-flooding experiment is shown in Figure 3. The experimental setup consisted of three containers with different fluids, a micro constant-speed displacement pump and a data collection system, a hydrostatic core holder, a pump to maintain core confining pressure, and a graduated cylinder for collecting fluid at the outlet. Firstly, the core was dried, vacuumed, and saturated with simulated formation water. Then, the crude oil was injected into the core at the rate of 0.1 mL/min until there was no water at the outlet. The irreducible water saturation was calculated, and the core was aged for 24 h at 50°C. After that, the simulated formation water was injected into the core at a rate of 0.1 mL/min until the water cut reached more than 98%, and the oil recovery of the water flood was calculated. The prepared Pickering emulsion system (0.3 PV) was injected at a rate of 0.1 mL/min. After the Pickering emulsion injection was completed, the extended water flooding was continued at a rate of 0.1 mL/min until the water cut reached 98%, and the EOR (Enhanced oil recovery) of the Pickering emulsion system was calculated. Refer to the production conditions of Daqing Oilfield, all flooding experiments were carried out at 50°C. The oil and water flow volume at the core outlet was continuously recorded during the experiment. The above experimental process was carried out on four cores with different permeabilities to analyze the influence of core permeability on the oil displacement efficiency.

3 Results

3.1 Characterization

The morphologies of Fe_3O_4@PDA@Si, Fe_3O_4@PDA, and Fe_3O_4 nanoparticles were determined by TEM and are shown in Figure 4. Comparing Figures 4A, B, D, E. it can be seen that PDA has been successfully coated on Fe_3O_4 nanoparticles, it can protect Fe_3O_4 nanoparticles from being oxidized, resulting in reduced magnetism. The Fe_3O_4@PDA nanoparticles exhibited an obvious core-shell structure. Comparing Figures 4B, C, E, F it can be seen that Fe_3O_4@PDA@Si nanoparticles have the same structure as Fe_3O_4@PDA nanoparticles, with a particle size of about 30 nm and a shell thickness of approximately 8 nm, indicating that the 1H, 1H, 2H, 2H-perfluorodecyltrichlorosilane only modifies the surface wettability of Fe_3O_4@PDA nanoparticles. To analyze the effect of dopamine and silane on the surface wettability, the water contact angles of Fe_3O_4, Fe_3O_4@PDA, and Fe_3O_4@PDA@Si nanoparticles were measured and are shown in Figures 4G–I. It can be found that the water contact angle of Fe_3O_4 nanoparticles is 35.9°, indicating that the Fe_3O_4 nanoparticles have strong hydrophilicity. After the dopamine was coated on Fe_3O_4

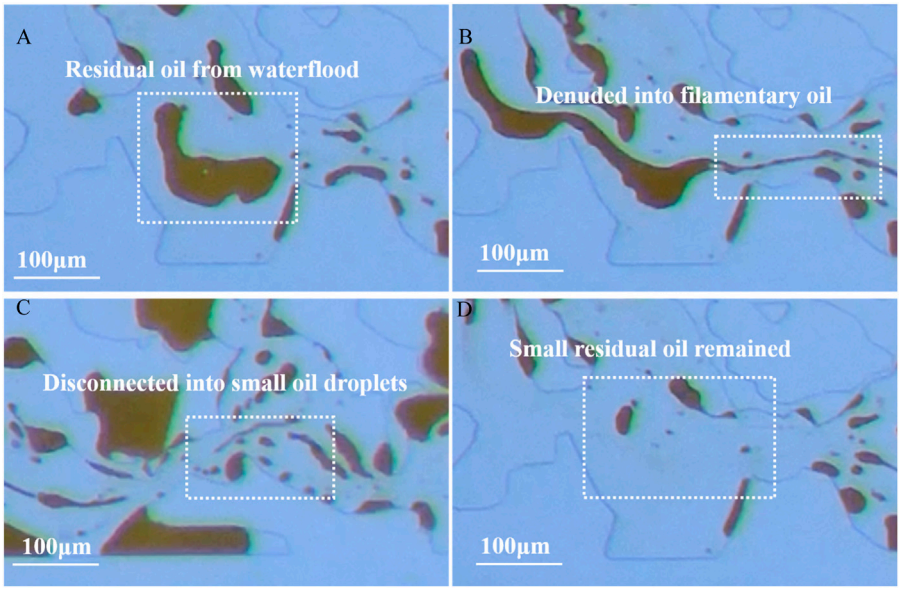

FIGURE 8
Emulsion denudation of residual oil in large pore during the Pickering emulsion injection: residual oil after waterflood in the pore **(A)**, partial residual oil stretched into filament **(B)**, filamentous oil broke into many small oil droplets **(C)**, and a little residual oil remained **(D)**.

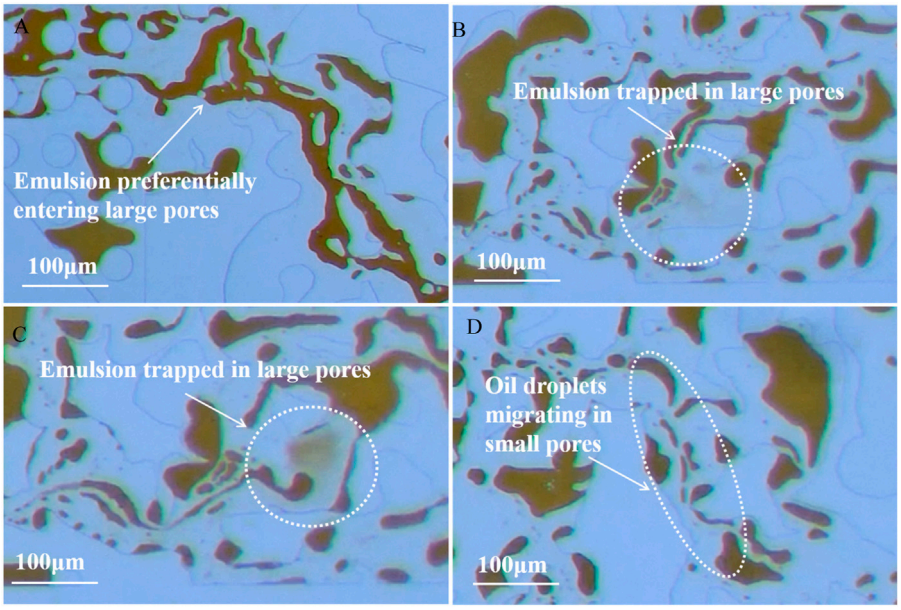

FIGURE 9
Profile control for residual oil during the Pickering emulsion flooding and extended waterflood: the Pickering emulsion preferentially entering large pores **(A)**, the Pickering emulsion trapped in large pores **(B, C)**, and oil droplets migrating in the small pores **(D)**.

nanoparticles, the water contact angle of Fe_3O_4@PDA nanoparticles is 38.1°, indicating that the dopamine does not influence the surface wettability of Fe_3O_4 nanoparticles. However, the water contact angle of Fe_3O_4@PDA@Si nanoparticles increases to 125.9° after the Fe_3O_4@PDA nanoparticles were modified by 1H, 1H, 2H, 2H-perfluorodecyltrichlorosilane. This is because the Fe_3O_4@PDA@Si nanoparticles contain more hydrophobic halogen groups (-F and -Cl groups), resulting in enhancing the hydrophobicity of Fe_3O_4@PDA@Si nanoparticles (Chen et al., 2018).

The crystal structure of Fe_3O_4, Fe_3O_4@PDA, and Fe_3O_4@PDA@Si nanoparticles were characterized by XRD and are shown in Figure 5A. It can be seen that Fe_3O_4, Fe_3O_4@PDA, and Fe_3O_4@

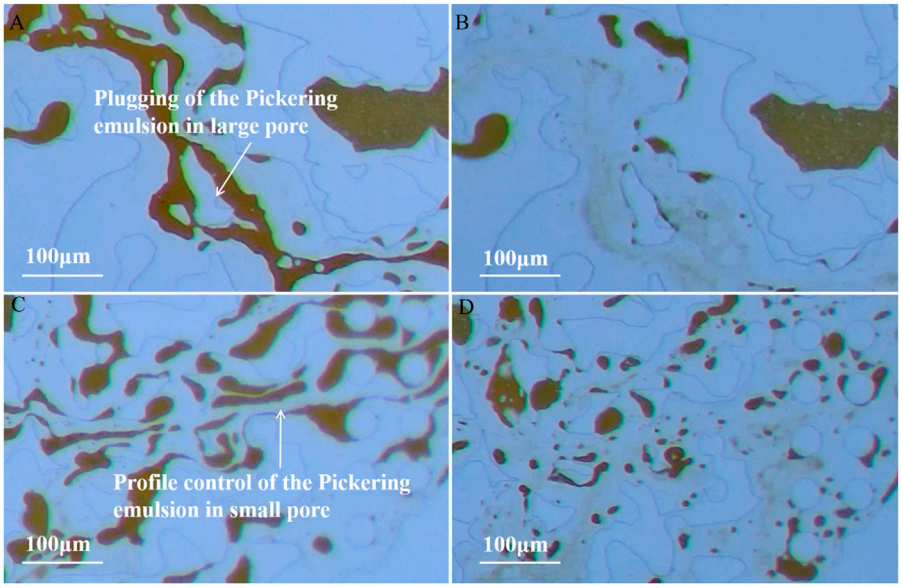

FIGURE 10
Residual oil distributions after the Pickering emulsion flooding **(A, C)** and extended waterflood **(B, D)** in different pores.

PDA@Si nanoparticles have the same diffraction peaks at 2θ = 18.28°, 30.12°, 35.42°, 43.12°, 53.60°, 56.96°, and 62.82°, compared with the standard Fe_3O_4 atlas PDF # 75–1,609, respectively corresponding to the lattice planes of (011), (112), (121), (004), (204), (231) and (400), indicating that the prepared Fe_3O_4 nanoparticles are a cubic spinel structure with sharp peak shape (Chen et al., 2021). It is preliminarily proved that Fe_3O_4 nanoparticles have been successfully prepared. The characteristic diffraction peaks of Fe_3O_4@PDA nanoparticles are consistent with those of Fe_3O_4 nanoparticles, indicating that the presence of PDA has no obvious effect on the crystal structure of Fe_3O_4 nanoparticles. The Fe_3O_4@PDA@Si nanoparticles have only the characteristic diffraction peaks of Fe_3O_4 without ones of Si. This may be due to the low content of silicon in the modifier or because the silicon was amorphous in the modifier.

The FTIR spectra of Fe_3O_4, Fe_3O_4@PDA, and Fe_3O_4@PDA@Si nanoparticles were measured and are shown in Figure 5B. The characteristic absorption peak of the Fe-O bond at 593 cm^{-1} is the absorption peak of Fe_3O_4, indicating that Fe_3O_4 nanoparticles were successfully obtained. The absorption peak at 3,414 cm^{-1} is formed by the hydroxyl or water adsorbed on the surface of Fe_3O_4 nanoparticles. Compared with the spectrum of Fe_3O_4 nanoparticles, it can be found that the O-H absorption peak moves from 3,414 cm^{-1} to 3,381 and 3,425 cm^{-1} in the spectra of Fe_3O_4@PDA and Fe_3O_4@PDA@Si nanoparticles, respectively. It shows that PDA and silane have a certain degree of influence on the hydroxyl groups on the surface of Fe_3O_4 nanoparticles. In the spectra of Fe_3O_4@PDA and Fe_3O_4@PDA@Si nanoparticles, a new absorption peak is observed at 2,925 cm^{-1} due to the presence of dopamine. In the spectrum of Fe_3O_4@PDA@Si nanoparticles, two new absorption peaks appear at 1,149 and 1,208 cm^{-1} corresponding to the asymmetric stretching vibration peak of Si-O-Si and the characteristic peak of -CH_3, respectively (Li et al., 2020). It is confirmed that dopamine and silane successfully coat on the surface of Fe_3O_4 nanoparticles.

3.2 Stability of pickering emulsions stabilized by Fe_3O_4@PDA@Si nanoparticles

The stability of the Pickering emulsions with different oil-water ratios was evaluated by measuring the water separating proportion and observing the microscopic morphology from the perspective of quantitative and qualitative analysis, as shown in Figure 6. As shown in Figures 6A, B, it can be observed that the final water separating proportion of the Pickering emulsion increases with an increase of the water phase volume. The water separating proportion of the Pickering emulsion is the lowest (6%) at the oil-water ratio of 5:5, which illustrates that the Pickering emulsion is the most stable at this oil-water ratio. On the one hand, the reason for this phenomenon may be that the larger the volume difference between the oil and water phases is, the more easily the phase with high proportion aggregates (Kazemzadeh et al., 2018). The structure of the Pickering emulsion is destroyed, resulting in an increase of the water separating proportion. On the other hand, it may be that the more the oil phase in the Pickering emulsion is, the higher the intensity of the oil-water interfacial film because the oil phase has greater viscoelasticity compared with the water phase (Ghaemi et al., 2015; Erdem and İşcan, 2021). Thus, the stability of the Pickering emulsion enhances with the increasing oil-water ratio. Conversely, the Pickering emulsion with more water phase is more unstable and has higher water separating proportion. In addition, as shown in Figure 6C, it is found that the Pickering emulsions with different oil-water ratios are all water-in-oil (W/O) type emulsions by observing the microscopic morphologies of the

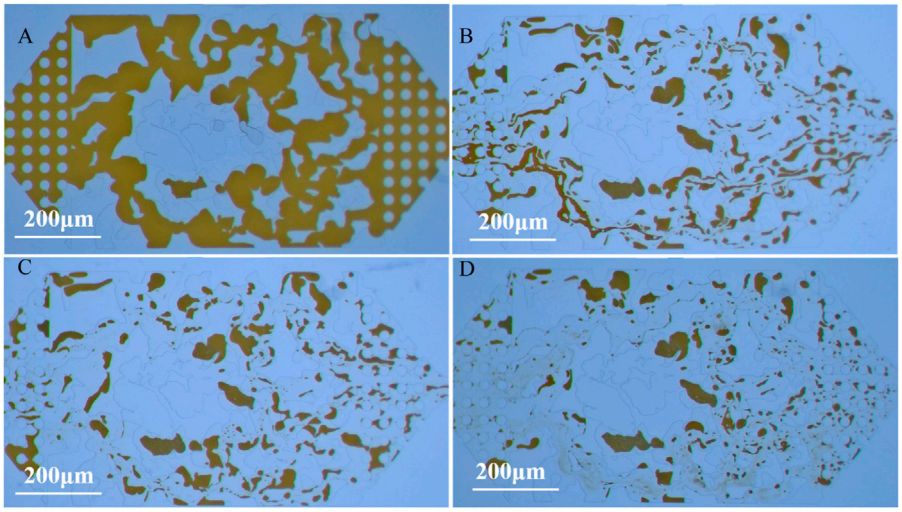

FIGURE 11
Initial Oil distribution **(A)** and residual oil distributions after water flooding **(B)**, Pickering emulsion flooding **(C)**, and extended waterflood **(D)** in the micromodel.

TABLE 2 Enhanced oil recovery (EOR) of the Pickering emulsion flooding in the micromodel.

Area	Oil recovery of waterflood (%)	EOR (%)		
		Pickering emulsion flooding	Extended waterflood	Pickering emulsion flooding and extended waterflood
Whole model	69.14	2.27	7.91	10.18

TABLE 3 Enhanced oil recovery (EOR) of the Pickering emulsion in cores with different permeabilities.

Core no.	Permeability (10^{-3} μm^2)	Porosity (%)	Initial oil saturation (%)	Oil recovery of waterflood (%)	Final oil recovery (%)	Incremental oil recovery (%)
1	219.34	21.05	69.87	57.69	75.08	17.39
2	365.28	23.89	72.08	60.85	76.47	15.62
3	537.92	24.63	75.69	63.18	77.21	14.03
4	834.86	24.27	78.35	65.26	77.62	12.36

TABLE 4 Effect of Pickering emulsion and Traditional emulsion on Tertiary Oil Recovery.

Flooding system	Incremental oil recovery (%)	Ref
DMSTNs-0.01 stabilized Pickering emulsion	14.05	Jia et al. (2021b)
GOJSC12 stabilized Pickering emulsion	14.8	Jia et al. (2022)
1% OP-10 emulsion	10.5	Feng et al. (2018)
0.1% OP-10 emulsion	6.72	Pei et al. (2017)

Pickering emulsions. The distribution of the emulsion droplets is very uneven at the oil-water ratio of 1:9 and 2:8 while the particle size of the emulsion droplets is nearly the same at the oil-water ratio of 5:5 and the droplets are arranged regularly throughout the field of view. It can be seen that the prepared Pickering emulsion at the oil-water ratio of 5:5 has the best stability.

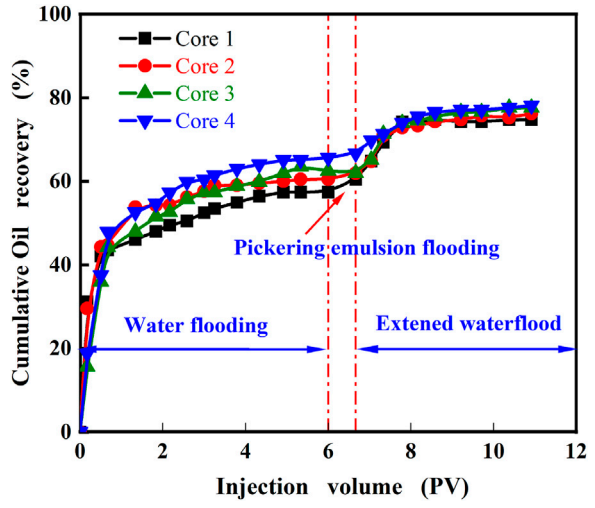

FIGURE 12
Curves of the cumulative oil recovery with the volume of the injected fluid in cores with different permeabilities.

3.3 Microscopic displacement characteristics of pickering emulsions stabilized by Fe_3O_4@PDA@Si nanoparticles

Fe_3O_4@PDA@Si nanoparticles with the percentage concentration of 0.5 wt% (mass fraction) were used to prepare the Pickering emulsion at the oil-water ratio of 5:5 for flow experiments. Microscopic flooding experiments were applied to investigate the microscopic displacement characteristics of the Pickering emulsion stabilized by Fe_3O_4@PDA@Si nanoparticles. In the microscopic displacement experiment, water flooding was carried out first and then a slug (0.3 PV) of the Pickering emulsion was injected at the residual oil saturation, followed by an extended water flooding. In the process of water flooding, there was a significant "viscous fingering" phenomenon due to the low resistance of the large pores. The injected water preferentially entered into the large pores, and only a small amount of water was driven into the small pores (Zhao et al., 2022). Thus, there was a large amount of residual oil in the micromodel after waterflood, as shown in Figure 7. It can be seen from the distribution pattern of residual oil in the micromodel after water flooding that the residual oil existed in the forms of column, membrane, cluster, and islet, as shown in Figures 7B, D. The residual oil in the small pores was mainly in the cluster and column forms while the residual oil in the membrane and column forms was mainly distributed in the large pores, with a small amount of the residual oil in form of islets, as shown in Figures 7A, C. Clustered residual oil continuously distributed in the small pores was the main form of residual oil distribution after water flooding (Fang et al., 2019).

The flow state of the residual oil after waterflood was observed and analyzed under the emulsification denudation during the Pickering emulsion flooding, as shown in Figure 8. As the Pickering emulsion entered into the micromodel, the residual oil started to migrate in large pores under the action of the emulsion (Figure 8A). Then, partial residual oil contacted with the Pickering emulsion gradually was elongated to form the filamentous oil due to the denudation of the emulsion (Figure 8B). After that, the filamentous oil separated from the original residual oil and turned into many small oil droplets under the continuous denudation (Figure 8C). The stripped oil droplets easily flowed out from the pore under displacement pressure. Finally, most of the residual oil was displaced and only a little residual oil remained in this pore (Figure 8D). Therefore, the Pickering emulsion can greatly reduce the saturation of residual oil in complex porous media by the emulsification denudation to improve the oil recovery.

The flow characteristics of the Pickering emulsion were investigated and shown in Figure 9 during the Pickering emulsion flooding and extended waterflood. The water entered into the large pore due to the low flow resistance to form the water flow predominant channel in porous medium during the waterflood (Gong et al., 2016). After the water broke through the water flow predominant channel where most of the crude oil was driven, a large amount of crude oil remained in the small pores. The Pickering emulsion preferentially entered into the water flow predominant channel during the subsequent Pickering emulsion flooding (Figure 9A). Due to high viscosity characteristic, the Pickering emulsion had a low mobility and moved slowly in large pores (Arab et al., 2018). In addition, the Pickering emulsion was easily trapped in large pores due to the complex throat structure of the porous medium (Figures 9B, C). As the extended waterflood commenced, the Pickering emulsion can plug the large pores and divert the subsequent water to enter into the small pores (Figure 9D). Thus, it can be seen that the Pickering emulsion can increase the swept volume of the subsequent water, which is beneficial for improving oil recovery.

The residual oil distributions after the Pickering emulsion flooding and extended waterflood in different pores were shown in Figure 10. After the Pickering emulsion flooding finished, the Pickering emulsion preliminarily achieved the plugging for large pores and the profile control for residual oil in small pores (Davoodi et al., 2022; Shi et al., 2023). The residual oil saturation in the pores only slightly decreases due to a little volume of the injected Pickering emulsion (Figures 10A, C). As the extended waterflood started, the swept volume of water greatly increased due to the plugging of the Pickering emulsion in large pores. A large amount of water entered into the small pores, resulting in a significant decrease of the residual oil saturation (Figures 10B, D). This indicates that the Pickering emulsion has a strong profile control effect on the residual oil in small pores with the increasing volume of the injected water.

To quantitatively investigate the enhanced oil recovery (EOR) of the Pickering emulsion, the photographs of the residual oil distribution were achieved and shown in Figure 11. Figure 11A shows the initial oil saturation in the whole micromodel. Figure 11B shows the residual oil distribution after waterflood. It was seen that there was a large amount of residual oil in the middle and inlet parts of the micromodel. Figure 11C shows the residual oil distribution after the injection of the Pickering emulsion. The Pickering

emulsion flowed first into the large pores and then switched into the small pores with an increase of the flow resistance in large pores. The plugging of the Pickering emulsion in large pores recovered a portion of the crude oil at the entrance of the micromodel (Xu et al., 2023). Figure 11D shows the residual oil distribution after the extended waterflood. The water was diverted into the small pores due to the plugging of the Pickering emulsion in large pores during the extended water flooding (He et al., 2022). Thus, the extended waterflood could recover a lot of residual oil in small pores. The four photographs were treated by the gray thresholds to calculate the residual oil saturation for EOR, as shown in Table 2. It can be seen that the EOR can reach 10.18% by the Pickering emulsion in the micromodel.

3.4 Enhanced oil recovery of pickering emulsions stabilized by Fe_3O_4@PDA@Si nanoparticles

Core-flooding experiments were carried out using the prepared Pickering emulsion in four cores with the permeabilities of 219.34, 365.28, 537.92, and 834.86 × 10^{-3} μm^2 to further investigate the ability of enhanced oil recovery of the Pickering emulsion stabilized by Fe_3O_4@PDA@Si nanoparticles. The results of core-flooding experiments with regard to incremental oil recovery are recorded in Table 3. It can be seen from Table 3 that when the permeability decreases from 834.86 to 219.34 × 10^{-3} μm^2, the incremental oil recovery of the Pickering emulsion increases from 12.36% to 17.39%, with an increase of 5.03%. From Table 4, it can be seen that compared to existing emulsion systems, Pickering emulsion stabilized by Fe_3O_4@PDA@Si nanoparticles has a good tertiary oil displacement effect. This indicates that the Pickering emulsion can effectively improve oil recovery through profile control plugging and emulsification denudation in porous medium, and the enhanced oil recovery of the Pickering emulsion in low permeability cores is better than that in high permeability cores.

The curves of the cumulative oil recovery with the volume of the injected fluid in four cores are shown in Figure 12. The oil recovery of water flooding increases first and then tends to be flat in each core. This is attributed to the "fingering" phenomenon occurs during the water flooding process, due to viscosity contrast between water and crude oil. After the Pickering emulsion is injected, the residual oil after water flooding is gradually eroded and separated from the surface of core pores due to the emulsification denudation of the Pickering emulsion (Khoramian et al., 2022). Thus, the cumulative oil recovery gradually increases with the increasing volume of the injected fluid. After extended waterflood is commenced, the swept volume of subsequent water is enlarged due to the plugging and profile control of the Pickering emulsion for large pores in cores, resulting in a further increase of the cumulative oil recovery. The incremental oil recovery of the Pickering emulsion in low permeability core is greater than that in high permeability core, illustrating that the plugging and profile control effect of the Pickering emulsion has a greater role in enhancing oil recovery, compared with the emulsification denudation.

4 Conclusion

In summary, Fe_3O_4@PDA@Si nanoparticles were successfully synthesized by coating and modifying Fe_3O_4 nanoparticles using dopamine hydrochloride and 1H, 1H, 2H, 2H-perfluorodecyltrichlorosilane. The morphology, crystal structure, chemical composition, and wettability of Fe_3O_4@PDA@Si nanoparticles were characterized by means of relevant techniques. The stability of the Pickering emulsion stabilized by Fe_3O_4@PDA@Si nanoparticles was evaluated at different oil-water ratios. The microscopic displacement mechanism and the ability of enhanced oil recovery (EOR) of the Pickering emulsion were investigated using an etched glass micromodel and artificial cores as complex porous media of the reservoir. The major conclusions are drawn as follows:

(1) Fe_3O_4@PDA@Si nanoparticles have an obvious core-shell structure, with a particle size of about 30 nm and a shell thickness of approximately 8 nm, with a water contact angle of 125.9°. The stability of the Pickering emulsion stabilized by Fe_3O_4@PDA@Si nanoparticles enhances with the increasing oil-water ratio. The Pickering emulsion at the oil-water ratio of 5: 5 has the best stability with the water separating proportion of only 6% and uniform distribution of the emulsion droplets with a particle size of about 15 μm.
(2) The Pickering emulsion stabilized by Fe_3O_4@PDA@Si nanoparticles can greatly reduce the residual oil in large pores by emulsification denudation. Meanwhile, the Pickering emulsion can plug the large pores and decrease the residual oil in small pores by the profile control to enhance oil recovery. The Pickering emulsion can achieve an enhanced oil recovery of 10.18% in the micro model.
(3) The incremental oil recovery of the Pickering emulsion increases with a decrease of core permeability. The incremental oil recovery increases from 12.36% to 17.39% when the core permeability decreases from 834.86 to 219.34 × 10^{-3} μm^2. The plugging and profile control effect of the Pickering emulsion has a greater role in improving oil recovery in low permeability core, compared with the emulsification denudation.
(4) In this work the Pickering emulsion system stabilized by Fe_3O_4@PDA@Si nanoparticles has high stability and excellent ability to improve oil recovery in both core and micro experiments. However, The preparation process of Fe_3O_4@PDA@Si nanoparticles cannot be achieved through one-step synthesis, future researchers can explore their synthesis process.

Data availability statement

The original contributions presented in the study are included in the article/supplementary material, further inquiries can be directed to the corresponding author.

Author contributions

XH conceived the idea and wrote the manuscript. YL, XG,YW, XH,JL, YX, BW, and FS contributed to the study and gave final approval for the manuscript. All authors contributed to the article and approved the submitted version.

Funding

This work has been financially supported by the Natural Science Foundation of Zhejiang Province (LY19A020004), the National Natural Science Foundation of China (12272350, 11602221), and the General Research Projects of Zhejiang Provincial Department of Education (Y202147649).

Acknowledgments

We would like to express our gratitude to the funding provided by the Zhejiang Provincial Natural Science Foundation (LY19A020004) and the National Natural Science Foundation of China (12272350,11602221), and we sincerely thank YL for his valuable guidance and support throughout the entire learning process.

Conflict of interest

Author GX was employed by the company China National Logging Corporation.

The remaining authors declare that the research was conducted in the absence of any commercial or financial relationships that could be construed as a potential conflict of interest.

Publisher's note

All claims expressed in this article are solely those of the authors and do not necessarily represent those of their affiliated organizations, or those of the publisher, the editors and the reviewers. Any product that may be evaluated in this article, or claim that may be made by its manufacturer, is not guaranteed or endorsed by the publisher.

References

AfzaliTabar, M., Alaei, M., Bazmi, M., Khojasteh, R. R., Koolivand-Salooki, M., Motiee, F., et al. (2017). Facile and economical preparation method of nanoporous graphene/silica nanohybrid and evaluation of its Pickering emulsion properties for Chemical Enhanced oil Recovery (C-EOR). *Fuel* 206, 453–466. doi:10.1016/j.fuel.2017.05.102

Arab, D., Kantzas, A., and Bryant, S. L. (2018). Nanoparticle stabilized oil in water emulsions: A critical review. *J. Petrol Sci. Eng.* 163, 217–242. doi:10.1016/j.petrol.2017.12.091

Bai, Y., Xiong, C., Shang, X., and Xin, Y. (2014). Experimental study on ethanolamine/surfactant flooding for enhanced oil recovery. *Energy & fuels* 28 (3), 1829–1837. doi:10.1021/ef402313n

Cao, J., Chen, Y., Xu, G., Wang, X., Li, Y., Zhao, S., et al. (2022). Study on interface regulation effects of Janus nanofluid for enhanced oil recovery. *Colloids Surfaces A* 653, 129880. doi:10.1016/j.colsurfa.2022.129880

Carvalho, M. S., and Alvarado, V. (2014). Oil recovery modeling of macro-emulsion flooding at low capillary number. *J. Petrol Sci. Eng.* 119, 112–122. doi:10.1016/j.petrol.2014.04.020

Chen, L., Zhang, G., Wu, G., Wang, P., Zhang, Y., Li, M., et al. (2021). Facile and environment-friendly mussel-inspired surface modification of PBO fibers via dopamine/3-aminopropyltrimethoxysilane co-deposition for advanced composite. *Polymer* 229, 123999. doi:10.1016/j.polymer.2021.123999

Chen, P., Cao, Z. F., Wang, S., and Zhong, H. (2018). *In situ* nano-silicate functionalized magnetic composites by (poly) dopamine to improve MB removal. *Colloids Surfaces A* 552, 89–97. doi:10.1016/j.colsurfa.2018.05.027

Cheraghian, G., Rostami, S., and Afrand, M. (2020). Nanotechnology in enhanced oil recovery. *Processes* 8 (9), 1073. doi:10.3390/pr8091073

Davoodi, S., Al-Shargabi, M., Wood, D. A., Rukavishnikov, V. S., and Minaev, K. M. (2022). Experimental and field applications of nanotechnology for enhanced oil recovery purposes: A review. *Fuel* 324, 124669. doi:10.1016/j.fuel.2022.124669

Erdem, B., and İşcan, K. B. (2021). Multifunctional magnetic mesoporous nanocomposites towards multiple applications in dye and oil adsorption. *J. Sol-Gel Sci. Techn.* 98, 528–540. doi:10.1007/s10971-021-05528-8

Fang, Y., Yang, E., and Cui, X. (2019). Study on distribution characteristics and displacement mechanism of microscopic residual oil in heterogeneous low permeability reservoirs. *Geofluids* 2019, 1–12. doi:10.1155/2019/9752623

Feng, H., Kang, W., Zhang, L., Chen, J., Li, Z., Zhou, Q., et al. (2018). Experimental study on a fine emulsion flooding system to enhance oil recovery for low permeability reservoirs. *J. Pet. Sci. Eng.* 171, 974–981. doi:10.1016/j.petrol.2018.08.011

Gbadamosi, A. O., Junin, R., Manan, M. A., Yekeen, N., Agi, A., and Oseh, J. O. (2018). Recent advances and prospects in polymeric nanofluids application for enhanced oil recovery. *J. Ind. Eng. Chem.* 66, 1–19. doi:10.1016/j.jiec.2018.05.020

Ghaemi, N., Madaeni, S. S., Daraei, P., Rajabi, H., Zinadini, S., Alizadeh, A., et al. (2015). Polyethersulfone membrane enhanced with iron oxide nanoparticles for copper removal from water: Application of new functionalized Fe_3O_4 nanoparticles. *Chem. Eng. J.* 263, 101–112. doi:10.1016/j.cej.2014.10.103

Gogoi, S., and Gogoi, S. B. (2019). Review on microfluidic studies for EOR application. *J. Pet. Explor Prod. Technol.* 9, 2263–2277. doi:10.1007/s13202-019-0610-4

Gong, H., Li, Y., Dong, M., Ma, S., and Liu, W. (2016). Effect of wettability alteration on enhanced heavy oil recovery by alkaline flooding. *Colloids Surfaces A* 488, 28–35. doi:10.1016/j.colsurfa.2015.09.042

He, J., Jia, H., Wang, Q., Xu, Y., Zhang, L., Jia, H., et al. (2022). Investigation on pH and redox-trigged emulsions stabilized by ferrocenyl surfactants in combination with Al_2O_3 nanoparticles and their application for enhanced oil recovery. *Colloids Surfaces A* 655, 130303. doi:10.1016/j.colsurfa.2022.130303

Jia, H., Dai, J., Miao, L., Wei, X., Tang, H., Huang, P., et al. (2021a). Potential application of novel amphiphilic Janus-SiO_2 nanoparticles stabilized O/W/O emulsion for enhanced oil recovery. *Colloids Surfaces A* 622, 126658. doi:10.1016/j.colsurfa.2021.126658

Jia, H., He, J., Xu, Y., Wang, T., Zhang, L., Fan, F., et al. (2021b). Synthesis of hybrid dendritic mesoporous silica titanium nanoparticles to stabilize Pickering emulsions for enhanced oil recovery. *Colloids Surfaces A* 628, 127237. doi:10.1016/j.colsurfa.2021.127237

Jia, H., Wang, D., Wang, Q., Dai, J., Wang, Q., Wen, S., et al. (2022). The synthesis of novel amphiphilic GOJS-Cn nanoparticles and their further application in stabilizing Pickering emulsion and enhancing oil recovery. *J. Pet. Sci. Eng.* 214, 110537. doi:10.1016/j.petrol.2022.110537

Kazemzadeh, Y., Dehdari, B., Etemadan, Z., Riazi, M., and Sharifi, M. (2019). Experimental investigation into Fe_3O_4/SiO_2 nanoparticle performance and comparison with other nanofluids in enhanced oil recovery. *Petrol Sci.* 16, 578–590. doi:10.1007/s12182-019-0314-x

Kazemzadeh, Y., Sharifi, M., and Riazi, M. (2018). Mutual effects of Fe_3O_4/chitosan nanocomposite and different ions in water for stability of water-in-oil (W/O) emulsions at low–high salinities. *Energ Fuel* 32 (12), 12101–12117. doi:10.1021/acs.energyfuels.8b02449

Khoramian, R., Kharrat, R., and Golshokooh, S. (2022). The development of novel nanofluid for enhanced oil recovery application. *Fuel* 311, 122558. doi:10.1016/j.fuel.2021.122558

Li, N., Li, T., Qiao, X. Y., Li, R., Yao, Y., and Gong, Y. K. (2020). Universal strategy for efficient fabrication of blood compatible surfaces via polydopamine-assisted surface-initiated activators regenerated by electron transfer atom-transfer radical polymerization of zwitterions. *Acs Appl. Mater Inter* 12 (10), 12337–12344. doi:10.1021/acsami.9b22574

Li, W., Jiao, B., Li, S., Faisal, S., Shi, A., Fu, W., et al. (2022a). Recent advances on pickering emulsions stabilized by diverse edible particles: Stability mechanism and applications. *Front. Nutr.* 738, 864943. doi:10.3389/fnut.2022.864943

Li, X., Yue, X. A., Zou, J., and Yan, R. (2022b). A novel method to characterize dynamic emulsions generation and separation of crude oil–water system. *Ind. Eng. Chem. Res.* 61 (30), 11124–11138. doi:10.1021/acs.iecr.2c01543

Liang, T., Hou, J. R., Qu, M., Xi, J. X., and Raj, I. (2022). Application of nanomaterial for enhanced oil recovery. *Petrol Sci.* 19 (2), 882–899. doi:10.1016/j.petsci.2021.11.011

Long, Y., Huang, X., Gao, Y., Chen, L., Song, F., and Zhang, H. (2019a). Swelling mechanism of core–shell polymeric nanoparticles and their application in enhanced oil recovery for low-permeability reservoirs. *Energ Fuel* 33 (4), 3077–3088. doi:10.1021/acs.energyfuels.9b00131

Long, Y., Wang, R., Zhu, B., Huang, X., Leng, Z., Chen, L., et al. (2019b). Enhanced oil recovery by a suspension of core-shell polymeric nanoparticles in heterogeneous low-permeability oil reservoirs. *Nanomaterials* 9 (4), 600. doi:10.3390/nano9040600

Mehranfar, A., and Ghazanfari, M. H. (2014). Investigation of the microscopic displacement mechanisms and macroscopic behavior of alkaline flooding at different wettability conditions in shaly glass micromodels. *J. Petrol Sci. Eng.* 122, 595–615. doi:10.1016/j.petrol.2014.08.027

Namin, A. R., Rajabi-Kochi, M., Rashidi, A., Yazdi, E., Montazeri, M., and Gharesheikhlou, A. A. (2023). Investigation of cation-assisted, chemically and thermally enhanced nitrogen-doped graphene nanofluid application as an efficient micro-emulsifier from EOR perspective. *Fuel* 335, 127033. doi:10.1016/j.fuel.2022.127033

Niebel, T. P., Heiligtag, F. J., Kind, J., Zanini, M., Lauria, A., Niederberger, M., et al. (2014). Multifunctional microparticles with uniform magnetic coatings and tunable surface chemistry. *RSC Adv.* 4 (107), 62483–62491. doi:10.1039/c4ra09698c

Pei, H., Zhang, G., Ge, J., Jiang, P., Zhang, J., and Zhong, Y. (2017). Study of polymer-enhanced emulsion flooding to improve viscous oil recovery in waterflooded heavy oil reservoirs. *Colloids Surfaces A* 529, 409–416. doi:10.1016/j.colsurfa.2017.06.039

Rezvani, H., Kazemzadeh, Y., Sharifi, M., Riazi, M., and Shojaei, S. (2019). A new insight into Fe_3O_4-based nanocomposites for adsorption of asphaltene at the oil/water interface: An experimental interfacial study. *J. Petrol Sci. Eng.* 177, 786–797. doi:10.1016/j.petrol.2019.02.077

Shalbafan, M., Esmaeilzadeh, F., and Vakili-Nezhaad, G. R. (2020). Enhanced oil recovery by wettability alteration using iron oxide nanoparticles covered with PVP or SDS. *Colloids Surfaces A* 607, 125509. doi:10.1016/j.colsurfa.2020.125509

Sharma, T., Iglauer, S., and Sangwai, J. S. (2016). Silica nanofluids in an oilfield polymer polyacrylamide: Interfacial properties, wettability alteration, and applications for chemical enhanced oil recovery. *Ind. Eng. Chem. Res.* 55 (48), 12387–12397. doi:10.1021/acs.iecr.6b03299

Shi, F., Wu, J., Li, Z., Zhao, B., Li, J., Tang, S., et al. (2023). Performance evaluation and action mechanism analysis of a controllable release nanocapsule profile control and displacement agent. *Polymers* 15 (3), 609. doi:10.3390/polym15030609

Su, X., Li, X., Li, J., Liu, M., Lei, F., Tan, X., et al. (2015). Synthesis and characterization of core–shell magnetic molecularly imprinted polymers for solid-phase extraction and determination of Rhodamine B in food. *Food Chem.* 171, 292–297. doi:10.1016/j.foodchem.2014.09.024

Suleimanov, B. A., Abbasov, H. F., and Ismayilov, R. H. (2022). Enhanced oil recovery with nanofluid injection. *Petrol Sci. Technol.*, 1–18. doi:10.1080/10916466.2022.2094959

Tiong, A. C. Y., Tan, I. S., Foo, H. C. Y., Lam, M. K., Mahmud, H. B., Lee, K. T., et al. (2023). Study on the synergism of cellulose nanocrystals and janus graphene oxide for enhanced oil recovery. *Geoenergy Sci. Eng.* 221, 111242. doi:10.1016/j.petrol.2022.111242

Umar, A. A., Saaid, I. B. M., Sulaimon, A. A., and Pilus, R. B. M. (2018). A review of petroleum emulsions and recent progress on water-in-crude oil emulsions stabilized by natural surfactants and solids. *J. Petrol Sci. Eng.* 165, 673–690. doi:10.1016/j.petrol.2018.03.014

Wu, J., and Ma, G. H. (2016). Recent studies of pickering emulsions: Particles make the difference. *Small* 12 (34), 4633–4648. doi:10.1002/smll.201600877

Xu, C., Zhang, H., Kang, Y., Zhang, J., Bai, Y., Zhang, J., et al. (2022). Physical plugging of lost circulation fractures at microscopic level. *Fuel* 317, 123477. doi:10.1016/j.fuel.2022.123477

Xu, C., Zhang, H., She, J., Jiang, G., Peng, C., and You, Z. (2023). Experimental study on fracture plugging effect of irregular-shaped lost circulation materials. *Energy* 276, 127544. doi:10.1016/j.energy.2023.127544

Yakasai, F., Jaafar, M. Z., Sidek, M. A., Bandyopadhyay, S., Agi, A., and Ngouangna, E. N. (2023). Co-precipitation and grafting of (3-Aminopropyl) triethoxysilane on Ferro nanoparticles to enhance oil recovery mechanisms at reservoir conditions. *J. Mol. Liq.* 371, 121007. doi:10.1016/j.molliq.2022.121007

Zhao, X., Zhao, Y., Wang, Z., Chen, B., Fang, S., Li, P., et al. (2022). Insight into the influence of morphology and structure of Fe_3O_4 nanoparticles on demulsification efficiencies. *J. Dispers. Sci. Technol.*, 1–12. doi:10.1080/01932691.2022.2025822

Zhou, H., Wang, X., Yu, K., Zhang, C., Li, H., and Du, Z. (2014). Preparation of multi-walled carbon nanotube/polyaniline/Fe_3O_4 composites. *Integr. Ferroelectr.* 154 (1), 159–165. doi:10.1080/10584587.2014.904706

Zhou, Y., Yin, D., Chen, W., Liu, B., and Zhang, X. (2019). A comprehensive review of emulsion and its field application for enhanced oil recovery. *Energy Sci. Eng.* 7 (4), 1046–1058. doi:10.1002/ese3.354

Zhu, J., Xie, S., Yang, Z., Li, X., Chen, J., Zhang, X., et al. (2021). A review of recent advances and prospects on nanocellulose properties and its applications in oil and gas production. *J. Nat. Gas. Sci. Eng.* 96, 104253. doi:10.1016/j.jngse.2021.104253